IEEE Access
Multidisciplinary | Rapid Review | Open Access Journal

Received July 26, 2018, accepted September 30, 2018, date of publication October 15, 2018, date of current version November 9, 2018.

Digital Object Identifier 10.1109/ACCESS.2018.2876175

An Adaptive OFDM Detection Strategy for Range and Doppler Spread Targets in Non-Gaussian Clutter

ZHEN DU, ZENGHUI ZHANG, (Member, IEEE), AND WENXIAN YU, (Member, IEEE)
Shanghai Key Laboratory of Intelligent Sensing and Recognition, School of Electronic Information and Electrical Engineering, Shanghai Jiao Tong University, Shanghai 200240, China

Corresponding author: Zenghui Zhang (zenghui.zhang@sjtu.edu.cn)

This work was partly supported by the National Key Research and Development Program of China under Grant 2016YFE0100400.

ABSTRACT Orthogonal frequency division multiplexing (OFDM) radar can obtain higher target detection performance than traditional single carrier frequency radar due to simultaneously multiple frequency measurements. Meanwhile, the detection performance can be further improved by utilizing both the range and Doppler distribution information for extended targets. In this paper, an OFDM detection strategy for range and Doppler spread targets in non-Gaussian clutter is proposed, which comprises a new generalized likelihood ratio test (GLRT) detector and an adaptive waveform design method. The deduced GLRT detector is an asymptotically optimal detector and has a constant false alarm rate property. Comparisons show that the GLRT detector outperforms other existed detectors, which use the range-only spread model or the point-like target model. Furthermore, by optimizing the transmitted weights corresponding to different subcarriers of the OFDM signal, an approximate 2-dB output signal-to-clutter ratio improvement is achieved, which benefits the target detection with a cognitive manner.

INDEX TERMS Spread targets detection, OFDM, adaptive waveform design, non-Gaussian clutter.

I. INTRODUCTION

Since the orthogonal frequency division multiplexing (OFDM) technique was proposed, it has become a widely used modulation scheme for wireless digital communications [1]. Meanwhile, on account of many outstanding properties of the OFDM signal such as 1) thumb-tack ambiguity function, 2) without range-Doppler coupling, 3) good ability against multipath interference, 4) simple structure generated by IFFT and separated by FFT, 5) orthogonality of subcarriers, 6) frequency diversity, etc., it has also been introduced in radar community [2]. The researches of OFDM radar mainly concentrate on the ambiguity function [3], [4], target detection [5], [6] and tracking [7], waveform design [3], [7], [8], synthetic aperture radar (SAR) adaptive signal processing [9], and fusion system of wireless communications and radar sensing [10]–[13]. In this paper, we only pay attention to the target detection problems, especially in non-Gaussian clutter.

Target detection against clutter and noise is a long-term topic in radar field. Nevertheless, the detection problem for OFDM signaling systems has not drawn much attention until recent several years [5], [6], [14]. The relevant research work can be concluded from three aspects, i.e., the transmitted waveform (signal carrier or multi-carrier), the target model (point-like, range-only spread, or range-Doppler spread), and the clutter distribution (Gaussian or non-Gaussian). Sen and Nehorai [5] proposed a detection strategy for OFDM radar with Gaussian clutter to determine the presence of a target contained in a particular range cell (i.e. point-like target). This measurement model was further developed in [6] considering the effects of multipath scenarios. Here the clutter was modeled as a complex wide sense stationary (WSS) Gaussian random process with zero mean value, which was also used in many manuscripts [7], [15]. However, this clutter model may not hold for high resolution radars (HRRs) that can resolute the target into several range cells, with a few isolated points [16].

In [17], due to the observation of spikes, the clutter statistics can be usually modeled as a spherically invariant random process (SIRP). In this circumstance, the clutter vector is expressed as a product form in which two components are contained: one is known as texture component which exhibits a greater decorrelation time [18] than the other component interpreted as speckle component with a rapid

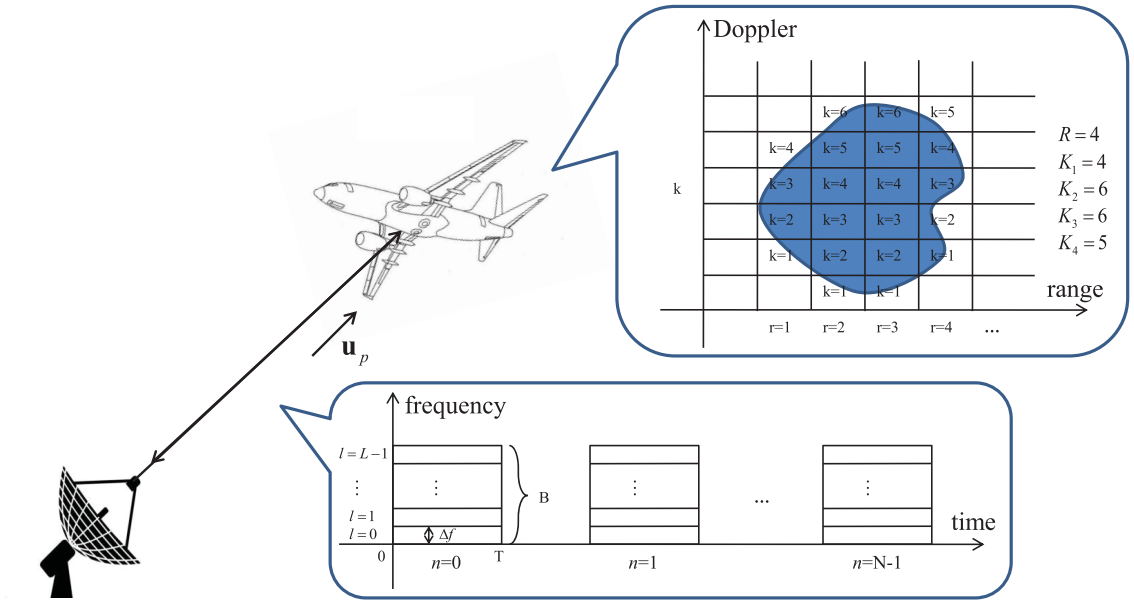

FIGURE 1. Diagram of the detection scenario. Upper block: target in the plane of range and Doppler; Lower block: time-frequency relationship of OFDM signal.

decorrelation time. This clutter model was also extensively used in [19]–[26]. In [14] a new OFDM detection strategy for point-like target model against non-Gaussian clutter was preliminarily investigated, ignoring the range and Doppler information of the target. Besides, by changing the complex transmitted weights of OFDM signal over different subcarriers to sense the surrounding environment, an adaptive waveform design method was proposed in [5], [6], and [14] so as to acquire a performance improvement. However, all the above detectors for OFDM radar were designed with the point-like target model. The problem of OFDM radar detection for range and Doppler spread targets is seldom mentioned in current researches.

On the other hand, there are many references about the detection of range and Doppler spread targets with the single carrier frequency radar waveform. In [27], Van Trees proposed two detectors for range spread and Doppler spread targets, respectively, in Gaussian clutter. For non-Gaussian clutter scenario, Gini studied the sub-optimal detector with a form of linear quadratic for fluctuating targets (e.g. Swerling I targets) in [21], and in [24] an adaptive detection strategy was further developed by replacing the covariance matrix with the matrix estimated from a set of ''secondary data'' collected from the range cells surrounding the cell under test (CUT). This method was also discussed in [22]. Gerlach [26] designed two constant false alarm rate (CFAR) detectors for range spread targets corresponding to the assumptions whether the target scatterers occupy all the range cells or not. Bon *et al.* [18] derived two CFAR detectors for range and Doppler spread targets considering two cases in which the complex amplitudes vector is 1) unknown but deterministic, 2) random with Gaussian disturbance. Simulation results demonstrate that the detection performance of these two detectors are very close.

We propose here to consider an adaptive OFDM detection strategy to determine the presence of range and Doppler spread targets against non-Gaussian clutter. The rest of this paper is organized as follows. In section II, the parametric measurement model is developed. Then, the clutter model is described and the GLRT detector is derived. After that, we compare our proposed GLRT detector with other designed detectors. In section III, an adaptive waveform design method is proposed, followed by numerical simulations and analyses in section IV. Conclusions are given in section V.

II. PROBLEM STATEMENT AND MODELING

In this section, we first develop a parametric measurement model of the received OFDM signal for a range and Doppler spread target. Then we consider the statistical characteristics of the non-Gaussian clutter modeled as a spherically invariant random vector (SIRV). After that, based on the Neyman-Pearson criterion, we derive an asymptotical optimum GLRT detector by replacing the unknown parameters with their ML estimations, which has previous CFAR property. At last, We also compare our proposed GLRT with some other detectors.

A. MEASUREMENT MODEL

We consider an OFDM detection strategy for a range and Doppler spread target against non-Gaussian clutter, of which the schematic representation is shown in Fig.1. The transmitted signal is with L active subcarriers,

a bandwidth of B Hz, and a pulse width of T seconds. Let $\Delta f = 1/T$ denote the subcarrier spacing, so as to keep the orthogonality of the OFDM signal. Thus, the complex envelope of the transmitted OFDM signal can be represented as

$$z(t) = \sum_{l=0}^{L-1} w_l e^{j2\pi l \Delta f t}$$

where w_l denotes the complex transmitted weight of the l-th subcarrier. The target is spatially distributed over R range cells, wherein every cell contains K_r scatterers. We use the subscript 'r' in K_r here to show that for different range cells the numbers of scatterers may not equal. We also consider the received signal at the output of the sensor with N sampling observations in a coherent pulse interval (CPI). The measurement signal $\boldsymbol{y}_r$ is composed of the signal echo $\boldsymbol{z}_r$ and the clutter vector $\boldsymbol{c}_r$. Therefore, the binary detection strategy is to distinguish between the following null hypothesis H_0 and the alternative hypothesis H_1

$$\begin{aligned} H_0 &: \boldsymbol{y}_r = \boldsymbol{c}_r \quad r = 1, 2, \cdots, R \\ H_1 &: \boldsymbol{y}_r = \boldsymbol{z}_r + \boldsymbol{c}_r \quad r = 1, 2, \cdots, R \end{aligned}$$

where $\boldsymbol{y}_r, \boldsymbol{z}_r$ and $\boldsymbol{c}_r \in \mathbb{C}^{LN}$ are $LN \times 1$ complex vectors. Thus, herein we have four variables

— time sampling index:n $\quad n = 0, 1, \cdots, N-1$
— subcarrier index:l $\quad l = 0, 1, \cdots, L-1$
— range cell index:r $\quad r = 1, 2, \cdots, R$
— Doppler scatterer index:k $\quad k = 1, 2, \cdots, K_r$

Then, the complex envelope of the signal echo at the output of the l-th subchannel for the k-th scatterer in the r-th range cell is formulated as [6]

$$z_{r,k,l}(n) = w_l x_{r,k,l} \phi_{r,k,l}(n)$$

where $\phi_{r,k,l}(n) = e^{-j2\pi f_l d_0} e^{j2\pi f_l \beta_{r,k} n T_{PRI}}$, and

— $x_{r,k,l}$ denotes the scattering coefficient of the l-th subcarrier for the k-th scatterer in the r-th range cell;
— $\beta_{r,k} = 2\langle \boldsymbol{v}_{r,k}, \boldsymbol{u}_p \rangle / c$, wherein $\beta_{r,k}$ is the relative Doppler shift along the DOA vector $\boldsymbol{u}_p$. $\boldsymbol{v}_{r,k}$ represents the velocity of the k-th scatterer in the r-th range cell, and c is the speed of light. And $\langle \cdot \rangle$ denotes inner product operator in Euclidean space.
— d_0 denotes the roundtrip delay. We assume that the relative time gaps among all the signal components are very small, compared with the actual roundtrip delay of the centroid of the target, i.e. $d_0 = d_{r,k,l}$; — $f_l = f_c + l\Delta f$ is the l-th subcarrier frequency and f_c is the carrier frequency;
— T_{PRI} is the pulse repetition interval.

Stacking all the subcarrier data into a $L \times 1$ dimension vector

$$\boldsymbol{z}_{r,k}(n) = \boldsymbol{W} \boldsymbol{\Phi}_{r,k}(n) \boldsymbol{x}_{r,k}$$

where

- $\boldsymbol{z}_{r,k}(n) = [z_{r,k,0}, z_{r,k,1}, \cdots, z_{r,k,L-1}]^{\mathrm{T}}$;
- $\boldsymbol{W} = \mathrm{diag}(w_0, w_1, \cdots, w_{L-1})$;
- $\boldsymbol{\Phi}_{r,k}(n) = \mathrm{diag}\left(\phi_{r,k,0}(n), \phi_{r,k,1}(n), \cdots, \phi_{r,k,L-1}(n)\right)$;
- $\boldsymbol{x}_{r,k} = [x_{r,k,0}, x_{r,k,1}, \cdots, x_{r,k,L-1}]^{\mathrm{T}}$.

Here, diag returns a square diagonal matrix with the elements of the vector on the main diagonal. we use '$^{\mathrm{T}}$' to denote the transpose operator and '$^{\mathrm{H}}$' in the following to denote the Hermitian operator.

Again stacking all the N sampling data into a $LN \times 1$ vector

$$\boldsymbol{z}_{r,k} = \boldsymbol{\Phi}_{r,k} \boldsymbol{x}_{r,k}$$

where

- $\boldsymbol{z}_{r,k} = [\boldsymbol{z}_{r,k}^{\mathrm{T}}(0), \boldsymbol{z}_{r,k}^{\mathrm{T}}(1), \cdots, \boldsymbol{z}_{r,k}^{\mathrm{T}}(N-1)]^{\mathrm{T}}$;
- $\boldsymbol{\Phi}_{r,k} = [(\boldsymbol{W}\boldsymbol{\Phi}_{r,k}(0))^{\mathrm{T}}, (\boldsymbol{W}\boldsymbol{\Phi}_{r,k}(1))^{\mathrm{T}}, (\boldsymbol{W}\boldsymbol{\Phi}_{r,k}(N-1))^{\mathrm{T}}]^{\mathrm{T}}$.

This arrangement of the received data is similar to that of array data, known as column rollout [28]. Then, we model the signal vector reflected by the r-th range cell, as a sum of all the K_r scatterers

$$\begin{aligned} \boldsymbol{z}_r &= \sum_{k=1}^{K_r} \boldsymbol{\Phi}_{r,k} \boldsymbol{x}_{r,k} = \boldsymbol{\Phi}_{r,1}\boldsymbol{x}_{r,1} + \boldsymbol{\Phi}_{r,2}\boldsymbol{x}_{r,2} + \cdots + \boldsymbol{\Phi}_{r,K_r}\boldsymbol{x}_{r,K_r} \\ &= [\boldsymbol{\Phi}_{r,1}, \boldsymbol{\Phi}_{r,2}, \cdots, \boldsymbol{\Phi}_{r,K_r}] \begin{bmatrix} \boldsymbol{x}_{r,1} \\ \boldsymbol{x}_{r,2} \\ \vdots \\ \boldsymbol{x}_{r,K_r} \end{bmatrix} \\ &= \boldsymbol{\Pi}_r \boldsymbol{x}_r \end{aligned} \tag{1}$$

where

- $\boldsymbol{\Pi}_r = [\boldsymbol{\Phi}_{r,1}, \boldsymbol{\Phi}_{r,2}, \cdots, \boldsymbol{\Phi}_{r,K_r}]$;
- $\boldsymbol{x}_r = [\boldsymbol{x}_{r,1}^{\mathrm{T}}, \boldsymbol{x}_{r,2}^{\mathrm{T}}, \cdots, \boldsymbol{x}_{r,K_r}^{\mathrm{T}}]^{\mathrm{T}}$.

The signal echo model in (1) is equivalent to the Gaussian linear model [28]. Then for convenience in the following subsections, we take the singular value decomposition (SVD), i.e. $\boldsymbol{\Pi}_r = \boldsymbol{U}_r \boldsymbol{S}_r \boldsymbol{V}_r^{\mathrm{H}}$, where $\boldsymbol{U}_r$ is the $LN \times LK_r$ unitary matrix of left singular vectors, $\boldsymbol{S}_r$ is the $LK_r \times LK_r$ diagonal matrix of non-zero singular values, and $\boldsymbol{V}_r$ is the $LK_r \times LK_r$ unitary matrix of right singular vectors. It is worth noting that the size of matrix $\boldsymbol{\Pi}_r$ cannot be too large due to the possible heavy burden of calculation with SVD. Thus, $\boldsymbol{z}_r$ can be equivalently modeled as

$$\boldsymbol{z}_r = \boldsymbol{U}_r \boldsymbol{b}_r$$

where $\boldsymbol{b}_r = \boldsymbol{S}_r \boldsymbol{V}_r^{\mathrm{H}} \boldsymbol{x}_r$. Thus, the detection problem can be reformulated as:

$$\begin{aligned} H_0 &: \boldsymbol{y}_z = \boldsymbol{c}_r \quad r = 1, 2, \cdots, R \\ H_1 &: \boldsymbol{y}_r = \boldsymbol{U}_r \boldsymbol{b}_r + \boldsymbol{c}_r \quad r = 1, 2, \cdots, R \end{aligned}$$

Based on the assumption that no priori knowledge is known about the distribution of $\boldsymbol{x}_r$, we can assume $\boldsymbol{b}_r$ to be an unknown deterministic vector. Consequently, for GLRT derivation we merely concern about the ML estimation of $\boldsymbol{b}_r$ regardless of the ML estimation of $\boldsymbol{x}_r$, as described in the following subsection. Besides, the signal subspace $\boldsymbol{U}_r$ is assumed to be priori known. For a realistic scenario, $\boldsymbol{U}_r$ can be estimated by signal subspace methods [18], which is beyond the scope of this paper.

B. CLUTTER MODEL

For low-range resolution radar, the clutter is usually assumed to be Gaussian distributed. For HRRs, due to the observation of spikes, the non-Gaussian clutter is modeled as a SIRP, a sample of which is a SIRV [17]. Then the non-Gaussian clutter vector $\boldsymbol{c}_r$ is expressed as a product in which two components are contained: one is known as texture component τ_r which exhibits a great decorrelation time, while the other component is interpreted as speckle component $\boldsymbol{s}_r$ with a rapid fluctuation time, that is

$$\boldsymbol{c}_r = \sqrt{\tau_r}\boldsymbol{s}_r \tag{2}$$

where

- $\boldsymbol{c}_r = [\boldsymbol{c}_r^{\mathrm{T}}(0), \boldsymbol{c}_r^{\mathrm{T}}(1), \cdots, \boldsymbol{c}_r^{\mathrm{T}}(N-1)]^{\mathrm{T}}$;
- $\boldsymbol{s}_r = [\boldsymbol{s}_r^{\mathrm{T}}(0), \boldsymbol{s}_r^{\mathrm{T}}(1), \cdots, \boldsymbol{s}_r^{\mathrm{T}}(N-1)]^{\mathrm{T}}$.

and for OFDM radar with L subcarriers

- $\boldsymbol{c}_r(n) = [c_{r,0}(n), c_{r,1}(n), \cdots, c_{r,L-1}(n)]^{\mathrm{T}}$;
- $\boldsymbol{s}_r(n) = [s_{r,0}(n), s_{r,1}(n), \cdots, s_{r,L-1}(n)]^{\mathrm{T}}$.

The clutter collected from the r-th range cell can be regarded as a result of many point scatterers producing incoherent reflections of the transmitted signal [5]. Thus, $\boldsymbol{s}_r(n)$ can be modeled as a L-dimensional Gaussian vector with zero-mean vector and positive definite covariance matrix $\boldsymbol{\Sigma}$ such that $\boldsymbol{s}_r(n) \sim \mathcal{CN}(\boldsymbol{0}, \boldsymbol{\Sigma})$. Also τ_r is constant over the N pulses and L subcarriers in the r-th range cell (i.e. $\tau_r = \tau_{r,k,l}$) because it exhibits a longer decorrelation time and is not affected by frequency agility [18]. This implies that

$$E[\boldsymbol{s}_r(n)\boldsymbol{s}_r^{\mathrm{H}}(n)] = \boldsymbol{\Sigma}$$
$$E[\boldsymbol{c}_r\boldsymbol{c}_r^{\mathrm{H}}] = \tau_r \cdot \boldsymbol{I}_N \otimes \boldsymbol{\Sigma} = \tau_r \cdot \boldsymbol{M}$$

where $\boldsymbol{I}_N$ represents the identity matrix of dimension N, $\boldsymbol{M} = \boldsymbol{I}_N \otimes \boldsymbol{\Sigma}$, and $\otimes$ denotes Kronecker product. It is obvious that the clutter is modeled as Gaussian distributed in the case of $r = 1$ (the point-like target is contained in a range cell) for low-range resolution radar. Therefore, the multivariate LNth-order probability density function (pdf) under the null hypothesis and alternative hypothesis can be determined as follows, respectively. Given a specific τ_r, thus the pdf under H_0 is

$$p(\boldsymbol{y}_{1:R} \mid_{\tau_{1:R}}, H_0) = \prod_{r=1}^{R} \frac{1}{\pi^{LN}\tau_r^{LN}|\boldsymbol{M}|} \exp\left(-\frac{\boldsymbol{y}_r^{\mathrm{H}}\boldsymbol{M}^{-1}\boldsymbol{y}_r}{\tau_r}\right)$$

and the pdf under H_1 is

$$p(\boldsymbol{y}_{1:R} \mid_{\tau_{1:R},\boldsymbol{U}_{1:R},\boldsymbol{b}_{1:R}}, H_1) = \prod_{r=1}^{R} \frac{1}{\pi^{LN}\tau_r^{LN}|\boldsymbol{M}|} \times \exp\left(-\frac{(\boldsymbol{y}_r - \boldsymbol{U}_r\boldsymbol{b}_r)^{\mathrm{H}}\boldsymbol{M}^{-1}(\boldsymbol{y}_r - \boldsymbol{U}_r\boldsymbol{b}_r)}{\tau_r}\right)$$

where $|\cdot|$ denotes the determinant operator. Herein the measured observations $\boldsymbol{y}_r, r = 1, 2, \cdots, R$ are assumed to be independent of each other. Moreover, we assume that the covariance matrix $\boldsymbol{M}$ is priori known. In practice, $\boldsymbol{M}$ is estimated thanks to a set of secondary data [21].

C. OPTIMUM DETECTOR AND GLRT

The NP detector can be expressed as [28]

$$\Lambda_{NP} = \frac{\prod_{r=1}^{R}\int_0^{\infty} p(\boldsymbol{y}_r \mid \boldsymbol{\tau}_r, H_1)p(\tau_r)d\tau_r}{\prod_{r=1}^{R}\int_0^{\infty} p(\boldsymbol{y}_r \mid \boldsymbol{\tau}_r, H_0)p(\tau_r)d\tau_r}$$

where $p(\tau_r)$ is the pdf of the random variable τ_r. However, due to the existence of the integrals in the formula of NP detector, it is rather computationally heavy to implement. In addition to that, we do not know the priori knowledge about $p(\tau_r)$ of the texture component. That is the reason we resort to a suboptimum approach based on GLRT where the unknown parameters $\boldsymbol{b}_r$, $\tau_{r|H_0}$ and $\tau_{r|H_1}$ are replaced by their ML estimates $\hat{\boldsymbol{b}}_r$, $\hat{\tau}_{r|H_0}$ and $\hat{\tau}_{r|H_1}$.

The ML estimates of τ_r under two hypotheses are respectively given by

$$\hat{\tau}_{r|H_0} = \frac{1}{LN}\boldsymbol{y}_r^{\mathrm{H}}\boldsymbol{M}^{-1}\boldsymbol{y}_r$$
$$\hat{\tau}_{r|H_1} = \frac{1}{LN}(\boldsymbol{y}_r - \boldsymbol{U}_r\boldsymbol{b}_r)^{\mathrm{H}}\boldsymbol{M}^{-1}(\boldsymbol{y}_r - \boldsymbol{U}_r\boldsymbol{b}_r)$$

The ML estimate of $\boldsymbol{b}_r$ under H_1 is given by

$$\hat{\boldsymbol{b}}_r = (\boldsymbol{U}_r^{\mathrm{H}}\boldsymbol{M}^{-1}\boldsymbol{U}_r)^{-1}\boldsymbol{U}_r^{\mathrm{H}}\boldsymbol{M}^{-1}\boldsymbol{y}_r$$

We follow the derive procedure in [18], i.e. substituting $\hat{\tau}_{r|H_1}$ and $\hat{\boldsymbol{b}}_r$ into $p(\boldsymbol{y}_{1:R} \mid_{\tau_{1:R},\boldsymbol{U}_{1:R},\boldsymbol{b}_{1:R}}, H_1)$, and $\hat{\tau}_{r|H_0}$ into $p(\boldsymbol{y}_{1:R} \mid_{\tau_{1:R}}, H_0)$,
then the GLRT is easily expressed by

$$\Lambda = N\sum_{r=1}^{R} \ln\left(\frac{\boldsymbol{y}_r^{\mathrm{H}}\boldsymbol{M}^{-1}\boldsymbol{y}_r}{\boldsymbol{y}_r^{\mathrm{H}}(\boldsymbol{M}^{-1} - \boldsymbol{Q}_r)\boldsymbol{y}_r}\right) \tag{3}$$

where $\boldsymbol{Q}_r = \boldsymbol{M}^{-1}\boldsymbol{U}_r(\boldsymbol{U}_r^{\mathrm{H}}\boldsymbol{M}^{-1}\boldsymbol{U}_r)^{-1}\boldsymbol{U}_r^{\mathrm{H}}\boldsymbol{M}^{-1}$ represents the orthogonal projection matrix onto the signal subspace $\boldsymbol{U}_r$. It is worth mentioning that the test statistic (3) is CFAR, which means the test is distribution free [21]–[24]. In fact, the detection threshold depends on the dimension (i.e. rank) of the orthogonal projection onto the whitening signal subspace $\widetilde{\boldsymbol{U}}_r = \boldsymbol{M}^{-1/2}\boldsymbol{U}_r$, see [18] for the detailed proof of CFAR property.

The above detector (3) is based on the model of non-Gaussian clutter. For comparison purpose, we further consider the Gaussian distributed clutter, i.e. $\boldsymbol{c}_r \sim \mathcal{CN}(\boldsymbol{0}, \sigma^2\boldsymbol{M})$, where σ^2 represents the mean power of the clutter. Then we discuss two cases.

Case 1: σ^2 is priori known. In this case by replacing the unknown parameter $\boldsymbol{b}_r$ with its ML estimate $\hat{\boldsymbol{b}}_r$ and then the GLRT is straightforward expressed as

$$\Lambda'(\boldsymbol{y}) = \exp\left(\frac{1}{\sigma^2}\sum_{r=1}^{R}\boldsymbol{y}_r^{\mathrm{H}}\boldsymbol{Q}_r\boldsymbol{y}_r\right) \gtrless \lambda$$

taking the logarithm and put the known constant σ^2 into the threshold λ, this detector can be rewritten as

$$\Lambda(\boldsymbol{y}) = \sum_{r=1}^{R}\boldsymbol{y}_r^{\mathrm{H}}\boldsymbol{Q}_r\boldsymbol{y}_r \gtrless \eta \tag{4}$$

where $\eta = \sigma^2\ln\lambda$.

Case 2: σ^2 is deterministic but unknown. In this case by replacing the unknown parameter $\boldsymbol{b}_r$, $\sigma^2_{|H_0}$ and $\sigma^2_{|H_1}$ with their ML estimates $\hat{\boldsymbol{b}}_r$, $\hat{\sigma}^2_{|H_0}$ and $\hat{\sigma}^2_{|H_1}$, then the GLRT is easily given by

$$\Lambda(\boldsymbol{y}) = \prod_{r=1}^{R} \left(\frac{\boldsymbol{y}_r^{\mathrm{H}} \boldsymbol{M}^{-1} \boldsymbol{y}_r}{\boldsymbol{y}_r^{\mathrm{H}} (\boldsymbol{M}^{-1} - \boldsymbol{Q}_r) \boldsymbol{y}_r} \right)^{N} \gtrless \eta \tag{5}$$

Remark 1: Notice that (5) is the same as (3) (by taking the logarithm of (5)), which indicates that based on our assumption (i.e. $\boldsymbol{b}_r$ is deterministic but unknown, the mean power σ^2 or τ_r of clutter is unknown, and the target is range and Doppler spread), the detection test is the same like (3) or (5) regardless of the statistical characteristics of clutter. Nonetheless, the detection performance differs remarkably for different clutter characteristics. For example, the performance of K-distributed clutter outperforms that of Gaussian clutter, which is discussed in the following numerical examples.

Remark 2: For the case of $r = 1$ (i.e. the target is entirely contained in one range cell), (4) is rewritten as

$$\Lambda(\boldsymbol{y}) = \boldsymbol{y}^{\mathrm{H}} \boldsymbol{Q} \boldsymbol{y} \gtrless \eta \tag{6}$$

while (5) is rewritten as

$$\Lambda(\boldsymbol{y}) = \frac{\boldsymbol{y}^{\mathrm{H}} \boldsymbol{M}^{-1} \boldsymbol{y}}{\boldsymbol{y}^{\mathrm{H}} (\boldsymbol{M}^{-1} - \boldsymbol{Q}) \boldsymbol{y}} \gtrless \eta^{1/N} \tag{7}$$

or transformed into another form

$$\Lambda(\boldsymbol{y}) = \boldsymbol{y}^{\mathrm{H}} \boldsymbol{Q} \boldsymbol{y} \gtrless \zeta \cdot \boldsymbol{y}^{\mathrm{H}} \boldsymbol{M}^{-1} \boldsymbol{y} \tag{8}$$

where $\boldsymbol{Q} = \boldsymbol{M}^{-1}\boldsymbol{U}(\boldsymbol{U}^{\mathrm{H}}\boldsymbol{M}^{-1}\boldsymbol{U})^{-1}\boldsymbol{U}^{\mathrm{H}}\boldsymbol{M}^{-1}$ and $\zeta = 1 - \eta^{-1/N}$. In comparison with (6) (i.e. the clutter is Gaussian distributed and σ^2 is priori known), (8) indicates that: for a single range cell target (i.e. point-like target), provided that the clutter is non-Gaussian, or Gaussian with unknown power, the only modification is to substitute a data-dependent threshold for a fixed threshold [22].

D. COMPARISON WITH OTHER DETECTORS

To show the advantages of the proposed detector, in this subsection we discuss three cases of the target distribution (i.e. range and Doppler spread targets, range spread targets and point targets) and their corresponding typical GLRT detectors in non-Gaussian clutter.

For low-range resolution radar, the target is entirely contained in one range cell because the size of target is smaller than the range resolution, leading to a point-like target model (i.e. $r = 1$). In this circumstance, Gini proposed a GLRT-linear quadratic (GLRT-LQ) detector [21], given by

$$|\boldsymbol{\Pi}^{\mathrm{H}} \boldsymbol{M}^{-1} \boldsymbol{y}|^2 \gtrless \lambda (\boldsymbol{y}^{\mathrm{H}} \boldsymbol{M}^{-1} \boldsymbol{y})(\boldsymbol{\Pi}^{\mathrm{H}} \boldsymbol{M}^{-1} \boldsymbol{\Pi}) \tag{9}$$

then (9) is equivalent to

$$\frac{|\boldsymbol{\Pi}^{\mathrm{H}} \boldsymbol{M}^{-1} \boldsymbol{y}|^2}{(\boldsymbol{y}^{\mathrm{H}} \boldsymbol{M}^{-1} \boldsymbol{y})(\boldsymbol{\Pi}^{\mathrm{H}} \boldsymbol{M}^{-1} \boldsymbol{\Pi})} \gtrless \lambda \tag{10}$$

Specifically, conventional optimum Gaussian detector (OGD) [28] is given by

$$|\boldsymbol{\Pi}^{\mathrm{H}} \boldsymbol{M}^{-1} \boldsymbol{y}|^2 \gtrless \lambda \tag{11}$$

Comparing (11) with (9), we find that the only modification is using a data dependent threshold in non-Gaussian clutter to replace a fixed threshold in Gaussian clutter, which coincides with the results of (6) and (8). In fact, (11) and (9) are equivalent to (6) and (8), respectively, depending on whether SVD is used in the derivative procedure or not.

As mentioned before, for HRRs we need to consider the range scale of the target because of the high range-resolution. In [26] Gerlach designed two constant false alarm rate (CFAR) detectors for range spread targets. Here we assume that the scatterers of target occupy all the range cells, thus Gerlach's GLRT detector is given by

$$\Lambda = -2(N-1) \sum_{r=1}^{R} \ln \left(1 - \underbrace{\frac{|\boldsymbol{\Pi}_r^{\mathrm{H}} \boldsymbol{M}^{-1} \boldsymbol{y}_r|^2}{(\boldsymbol{y}_r^{\mathrm{H}} \boldsymbol{M}^{-1} \boldsymbol{y}_r)(\boldsymbol{\Pi}_r^{\mathrm{H}} \boldsymbol{M}^{-1} \boldsymbol{\Pi}_r)}}_{\boldsymbol{G}} \right) \tag{12}$$

It is worth mentioning that $\boldsymbol{G}$ in (12) is obviously equivalent to (10) in the case of $r = 1$ because Λ increases monotonously with the increasing $\boldsymbol{G}$.

Also for range and Doppler spread targets Bon proposed DSM-GLRT [18], based on the assumption that the complex amplitudes vector is deterministic and unknown, which is given by

$$\Lambda = N \sum_{r=1}^{R} \ln \left(\frac{\boldsymbol{y}_r^{\mathrm{H}} \boldsymbol{M}^{-1} \boldsymbol{y}_r}{\boldsymbol{y}_r^{\mathrm{H}} (\boldsymbol{M}^{-1} - \boldsymbol{Q}_r) \boldsymbol{y}_r} \right) \tag{13}$$

It shows that (13) has the same form as (3). Nevertheless, Bon's detector is designed for single-carrier signal, and $\boldsymbol{\Pi}_r$ is of dimension $N \times K_r$, which can be regarded as a special case of $L = 1$, while our proposed detector is designed for multi-carrier signal of which $\boldsymbol{\Pi}_r$ is of dimension $LN \times LK_r$.

We summarized the comparison between our proposed detector and other detectors. All the above detectors could be viewed as the typical detectors according to the different types of targets. For OFDM signal, especially in non-Gaussian clutter, the existing literatures tell less about that. In Table 1, due to the characteristic of frequency diversity for OFDM signal, an adaptive waveform design method can be considered as stated in section III, which is the key distinction from Bon's detector. For range-only spread targets and point-like targets detection against non-Gaussian clutter with OFDM radar, we cannot directly take advantage of Gerlach's and Gini's detectors, respectively, of which essentially the reason is the dimensional limitation of OFDM signal (i.e. $L \geq 1$). Also in Table 1, the derivative procedures of our proposed and Bon's detectors include the use of SVD for convenience, exactly opposite to those of Gerlach's, Gini's detectors and OGD. Besides, we emphasize that all the detectors listed in Table 1 have CFAR properties.

TABLE 1. Comparison with other detectors. For space-saving purpose, we use some abbreviations in this table. Herein 'RD' represents range and Doppler spread targets, 'R' represents range-only spread targets and 'P' represents point-like targets. 'OGD' is the abbreviation of the optimum Gaussian detector.

	Detector	Target	Clutter	Dimension	Adaptive waveform design	SVD	CFAR
Our proposed	$N\sum_{r=1}^{R}\ln\left(\frac{\boldsymbol{y}_r^{\mathrm{H}}M^{-1}\boldsymbol{y}_r}{\boldsymbol{y}_r^{\mathrm{H}}(M^{-1}-\boldsymbol{Q}_r)\boldsymbol{y}_r}\right)$	RD	non-Gaussian	$L\geq 1$	$\surd$	$\surd$	$\surd$
Bon's [18]	$N\sum_{r=1}^{R}\ln\left(\frac{\boldsymbol{y}_r^{\mathrm{H}}M^{-1}\boldsymbol{y}_r}{\boldsymbol{y}_r^{\mathrm{H}}(M^{-1}-\boldsymbol{Q}_r)\boldsymbol{y}_r}\right)$	RD	non-Gaussian	$L=1$	$\times$	$\surd$	$\surd$
Gerlach's [26]	$-2(N-1)\sum_{r=1}^{R}\ln\left(1-\frac{\lvert\boldsymbol{\Pi}_r^{\mathrm{H}}M^{-1}\boldsymbol{y}_r\rvert^2}{(\boldsymbol{y}_r^{\mathrm{H}}M^{-1}\boldsymbol{y}_r)(\boldsymbol{\Pi}_r^{\mathrm{H}}M^{-1}\boldsymbol{\Pi}_r)}\right)$	R	non-Gaussian	$L=1$	$\times$	$\times$	$\surd$
Gini's [21]	$\frac{\lvert\boldsymbol{\Pi}^{\mathrm{H}}M^{-1}\boldsymbol{y}\rvert^2}{(\boldsymbol{y}^{\mathrm{H}}M^{-1}\boldsymbol{y})(\boldsymbol{\Pi}^{\mathrm{H}}M^{-1}\boldsymbol{\Pi})}$	P	non-Gaussian	$L=1$	$\times$	$\times$	$\surd$
OGD [28]	$\lvert\boldsymbol{\Pi}^{\mathrm{H}}\boldsymbol{M}^{-1}\boldsymbol{y}\rvert^2$	P	Gaussian	$L=1$	$\times$	$\times$	$\surd$

III. ADAPTIVE WAVEFORM DESIGN

In this section, we address an adaptive waveform design method to optimize the transmitted weights vector $\boldsymbol{w}$, where $\boldsymbol{w}=\mathrm{diag}(\boldsymbol{W})$, for the next CPI, so as to match the scattering coefficients and consequently improve the output signal to clutter ratio (SCR) and acquire a performance improvement.

For a point-like target contained in a range cell, the clutter is usually modeled as multivariate Gaussian distribution with OFDM radar. Therefore the detection problem is to evaluate the similarity between two multivariate Gaussian distribution with zero-mean vector and nonzero-mean vector, respectively. A usually solution is to maximize noncentrality parameter [5], i.e. the Mahalanobis distance [14]. This problem can be translated into a Rayleigh quotient and thus the optimized transmitted weights vector $\boldsymbol{w}$ is easily calculated. Nevertheless, we may not utilize the same approach [5], [6], [14] in our model on account of the complexity of the target with spatial and Doppler scales. From another perspective, we notice that the detection performance is monotonously increased with increasing output SCR. Thus, we consider to directly maximize the output SCR subject to a predefined energy constraint of $\boldsymbol{w}$, formulated as

$$\begin{cases}\boldsymbol{w}_{opt}=\underset{\boldsymbol{w}}{\mathrm{argmax}}\dfrac{\sum_{r=1}^{R}\left(\boldsymbol{\Pi}_r\left(\boldsymbol{w}\right)\boldsymbol{x}_r\right)^{\mathrm{H}}\left(\boldsymbol{\Pi}_r\left(\boldsymbol{w}\right)\boldsymbol{x}_r\right)}{\sum_{r=1}^{R}\boldsymbol{c}_r^{\mathrm{H}}\boldsymbol{c}_r}\\ \text{subject to}\quad \boldsymbol{w}^{\mathrm{H}}\boldsymbol{w}=1\end{cases}\tag{14}$$

Herein, we set a predefined energy constraint of $\boldsymbol{w}$ equal to 1, indicating that the power of transmitted signal is fixed. We use $\sum_{r=1}^{R}\boldsymbol{c}_r^{\mathrm{H}}\boldsymbol{c}_r$ to represent the total energy of received data of clutter, due to the different power levels of each range cell.

For this problem, an optimized transmitted weights vector $\boldsymbol{w}_{opt}$ is acquired for pulses in the next CPI. To solve (14) numerically, we resort to some optimization techniques, for instance, the optimization toolbox in [29] and [30].

IV. NUMERICAL EXAMPLES

In (2), the texture value τ_r represents the partial power of clutter in the r-th range cell. It can be assumed to be Gamma distributed with the shape parameter ν and the mean value μ

$$p(\tau_r)=\frac{1}{\Gamma(\nu)}\left(\frac{\nu}{\mu}\right)^{\nu}\tau_r^{\nu-1}e^{-\frac{\nu}{\mu}\tau_r}\quad \tau_r\geq 0$$

where $\Gamma(\cdot)$ is the Gamma function. The mean value is $E(\tau_r)=\mu$ and the variance is $E[(\tau_r-\mu)^2]=\mu^2/\nu$. Also $\boldsymbol{s}_r\sim\mathcal{CN}(\boldsymbol{0},\boldsymbol{M})$, as mentioned in section II. Then the clutter can be interpreted by the well-known K-distributed characteristics, see [16]–[26] for more references.

In the presence of K-distributed clutter, both the false alarm probability and detection probability cannot be obtained in a closed form, that is why we resort to standard Monte Carlo trials. We list all the following parameters of numerical examples. Unless specially mentioned, the parameters of these examples are the same.

- The carrier frequency of OFDM transmitted signal is set to be 1GHz with a bandwidth of $B=100$ MHz, and with $L=5$ subcarriers. Thus the sub-bandwidth is $\Delta f=B/L=20$MHz, and the pulse width is $T_p=1/\Delta f=50$ns;
- We assume that the target is spatially partitioned into $R=4$ range cells, and several numbers of scatterers in each cell are listed in Table 2, as Fig.2 intuitively shows the spatial and Doppler scales of the target. The target is located in a distance of 5 kilometers from the radar platform. The location can be easily extended to be a 2-D or 3-D detection scenario;

TABLE 2. Range and Doppler spread target parameters.

Cell	1	2	3	4
Velocity(m/s)	{15}	{15,30}	{15.30,45}	{15,30}

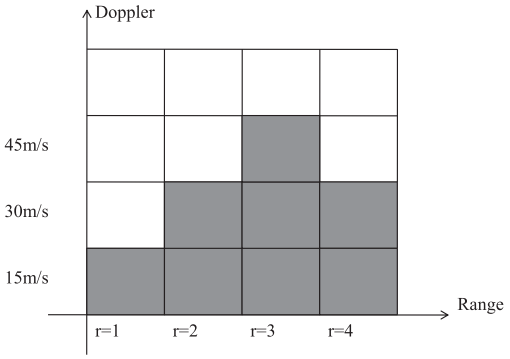

FIGURE 2. Diagram of the spatial and Doppler scales of the target.

- The clutter is assumed to be K-distributed with $\mu = 0.5$ and $\nu = 0.5$. The covariance matrix $\boldsymbol{M}$ is assumed to be an identity matrix of dimension $LN \times LN$. The fixed signal to clutter ratio is SCR $= -15$dB;
- We assume a CPI contains $N = 8$ pulses, and the pulse repetition interval is $T_{PRI} = 1$ms;
- The Monte Carlo simulation is based on 5000 independent trials.

A. CFAR PROPERTY

In Fig.3 a plot of probability of false alarm versus the threshold level in K-distributed clutter with different parameters is investigated. Note that $\nu = 0.1$ means very spiky K-distributed clutter, and $\nu = 4.5$ means almost Gaussian clutter. The results imply that the probability of false alarm is exceeding insensitive to the variation of shape parameter ν and mean value μ. The curves in Fig.3 are almost the same and merely have slight differences such that the detector is regarded to be CFAR, or even if it is not perfectly CFAR, it is very robust.

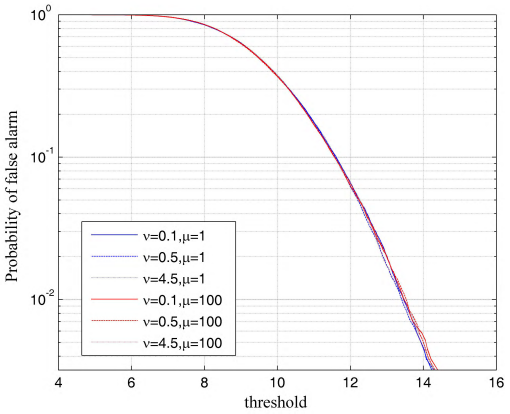

FIGURE 3. False alarm probability versus threshold level for different shape parameters ν and mean values μ of K-distributed clutter.

B. INFLUENCE OF DIFFERENT NUMBERS OF SUBCARRIERS AND SAMPLING PULSES

In Fig.4 it is evident that with the number of subcarriers increasing, the detection performance is largely improved,

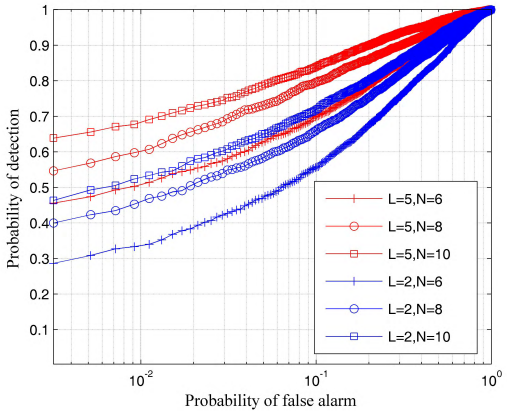

FIGURE 4. Receiver operating characteristics (ROC) curves for different numbers of subcarriers and sampling pulses in OFDM signaling systems.

which illustrates the advantage of using OFDM signal system due to frequency diversity. It is also implied that the detection performance has an obvious improvement when more sampling pulses are used in a CPI. Interestingly, with more sampling pulses N, the level of performance gain is becoming lower. In fact, when L becomes larger, the level of probability of detection gain is also increasing more slowly, because the spectrum of OFDM signal gradually closes to flat with an increasing L and finally has a rectangle shape, provided that $w_l = 1/\sqrt{L}$ for $l = 0, 1, \cdots, L-1$, which is not displayed in Fig.4.

C. INFLUENCE OF SHAPE PARAMETER OF K-DISTRIBUTED CLUTTER

When the shape parameter ν is larger, the clutter becomes more Gaussian. In practice, when $\nu > 10$ the clutter can be considered to be Gaussian-distributed [21]. In Fig.5 it is plotted ROC of different shape parameters in K-distributed clutter. It is obvious that the probability of detection can be remarkably improved by decreasing shape parameter ν, which means the spikier clutter corresponds to the better detection performance.

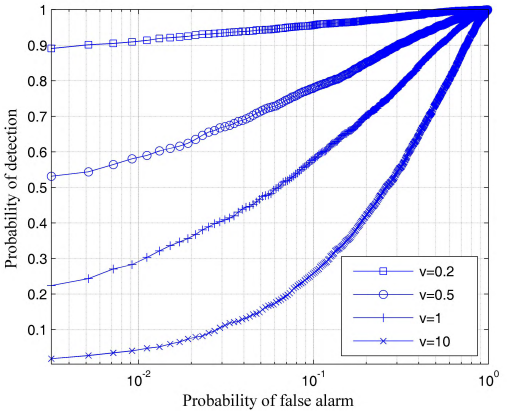

FIGURE 5. Receiver operating characteristics (ROC) curves for different shape parameters in K-distributed clutter.

D. INFLUENCE OF DIFFERENT CLUTTER STATISTICAL CHARACTERISTICS

We have shown that the detector statistics is of the same form regardless of the statistical characteristics of clutter and consequently we can directly compare the detection performance in different clutter. In Fig.6 it is showed that the detector performs much better in K-distributed clutter compared with Gaussian-distribution clutter in accordance with the same SCR value. The conclusion coincides with the result in Fig.5. In addition to that, it also shows the detection performance improves as SCR increases, as expected.

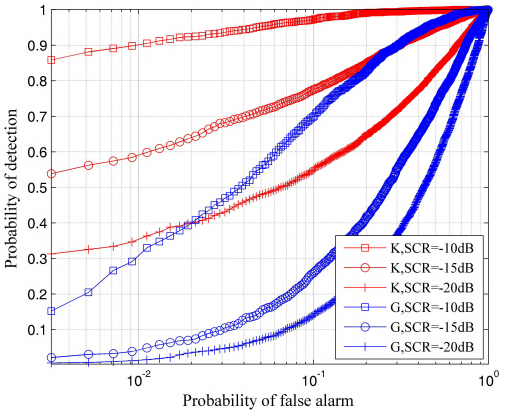

FIGURE 6. Receiver operating characteristics (ROC) curves for different SCR values under K-distributed (K, for short) and Gaussian (G, for short) clutter, respectively.

E. INFLUENCE OF CLUTTER TO NOISE RATIO (CNR)

In reality the measurement signal contains not only the signal echo and clutter, but also the noise generated by the receiver. In this subsection, we investigate the influence of additive noise in a clutter-dominant scenario. In this numerical example we add the data of white Gaussian noise (WGN) to the distributed vectors. The CNR is defined as

$$\mathrm{CNR} = \frac{\frac{1}{N}\sum_{r=1}^{R} \boldsymbol{c}_r^{\mathrm{H}} \boldsymbol{c}_r}{R\sigma_n^2}$$

where σ_n^2 is the average power of the noise in each range cell. In Fig.7 it demonstrates that the detection probability is considerably improved when CNR is increased. We set CNR equal to $+\infty$ and $-\infty$, corresponding to the upper bound and lower bound of the detection performance. In practice, when CNR is larger than 20dB, the performance nears the condition of that without noise, which implies the noise can be ignored. And when CNR is smaller than -10dB, the performance of detection seriously deteriorates, and gets close to the lower bound (i.e. the worst situation).

F. COMPARISON WITH OTHER DETECTORS

As mentioned before, due to the dimensional limitation, we cannot directly resort to Gerlach's and Gini's detectors for OFDM radar, respectively. For the case of range-only

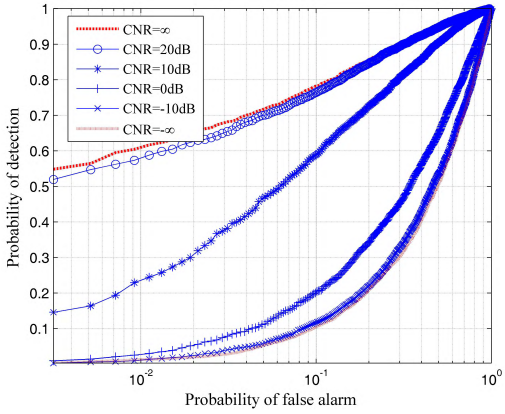

FIGURE 7. Receiver operating characteristics (ROC) curves for different clutter to noise ratio (CNR) values in a clutter dominant scenario.

spread targets, the test statistic is still expressed by (3), but the dimension of $\boldsymbol{\Pi}_r$ turns from $LN \times LK_r$ into $LN \times L$. For the case of point-like targets, the test statistic can be expressed by (7). Both these two detectors can be considered as the special cases of (3) for range and Doppler spread targets.

In this numerical example, firstly we plotted the ROC curves for the range and Doppler spread target by taking advantage of (3). For range-only spread designed detector, $K_r = 1$ for $r = 1, 2, \cdots, R$ where the velocity of each range cell is 15m/s in accordance with Table 2. Also for point target detector, the number of range cells is $R = 1$ and therefore we assume the received data is fully acquired from the first range cell with velocity of 15m/s. In Fig.8, all these three cases are considered. The results show that range-only spread designed detector in high range resolution radar has an immense performance gain compared with point target detector. In addition, by taking advantage of the information of Doppler frequencies, the detection performance can be remarkably improved again. We also plotted the ROC curves

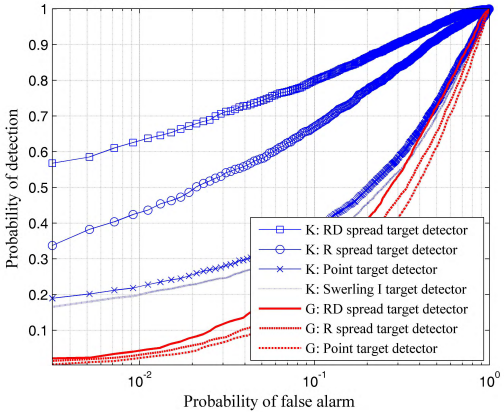

FIGURE 8. Receiver operating characteristics (ROC) for three different detectors: range and Doppler (RD, for short) designed detector, range-only (R, for short) spread designed detector, and point target detector. In addition to that, Swerling I designed detector is also considered. 'K' represents K-distributed clutter and 'G' represents Gaussian clutter.

for Swerling I target with fluctuated amplitudes, different from those with constant amplitudes set in the former numerical examples. The fluctuated amplitudes was realized from a Gaussian distribution with zero-mean value and variance of unit. The result in Fig.8 shows that amplitudes fluctuations give rise to a slight performance degradation, compared to the point target detector with constant amplitudes.

We also considered the three detectors in Gaussian clutter, which coincides with the results in Fig.6. Unlike the cases in K-distributed clutter, the detection performance has merely a slight gain for range and Doppler designed detector in Gaussian clutter, outperforming the other two detectors.

G. ADAPTIVE WAVEFORM DESIGN

Due to the frequency diversity, we can modify the transmit weight vector under a constraint condition to match the scattering coefficients and obtain the improved detection performance. To illustrate the advantage of adaptive waveform design method as proposed in (14), we followed the same comparison strategy in [5], [6], and [14]. For an adaptive system, we first set a predefined energy constraint of $\boldsymbol{w}$ equal to 1, as the constraint condition in (14) shows. Therefore, we transmitted $w_l = 1/\sqrt{L}$ for $l = 1, 2, \cdots, L$ in the first CPI, and then took advantage of (14) to calculate and transmit the optimized $\boldsymbol{w}_{opt}$ for the second CPI, in comparison with a fixed system in which both CPIs transmit $w_l = 1/\sqrt{L}$ for $l = 1, 2, \cdots, L$.

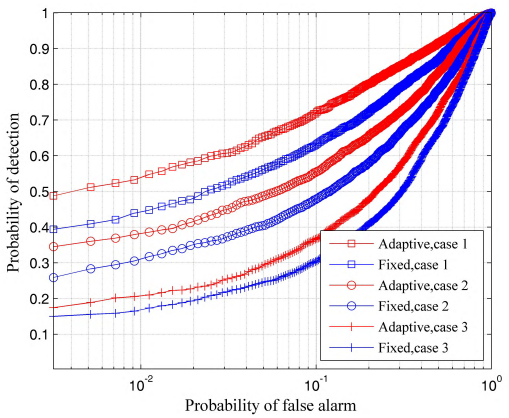

FIGURE 9. Receiver operating characteristics (ROC) for fixed waveform and adaptive waveform. Three cases are considered according to different SCR values set for fixed waveform.

In this subsection, for a fair comparison, we set the same transmitted power for adaptive waveform and fixed waveform. However, it is noted that the noise power is always fixed. We chose three different values of the transmitted power in this numerical example, respectively, corresponding to the three cases in Fig.9. Thus, at the receiver, the SCR value can be calculated by the average of 5000 Monte Carlo trails. The calculated results of SCR for both fixed waveform and adaptive waveform in three cases are listed in Table 3. The data in Table 3 shows that the detection performances in three cases are all improved after adaptive waveform design, due to an improvement of SCR, approximately equal to 2dB improvement. Interestingly, for case 3, the gain of SCR is larger than 2dB while the improvement of probability of detection is obviously smaller than those in case 1 and case 2, approximately equal to 0.1 of probability of detection gain. It is due to the nonlinear relationship between the probability of detection and SCR. And it may imply that adaptive waveform design has a more remarkable effect on larger SCR values.

TABLE 3. The SCR values calculated by the average of 5000 Monte Carlo trails for fixed waveform and adaptive waveform in three cases.

	case 1	case 2	case 3
fixed waveform	-16.52dB	-19.91dB	-25.93dB
adaptive waveform	-14.51dB	-17.92dB	-23.86dB

V. CONCLUSION

We addressed an adaptive OFDM detection strategy for a range and Doppler spread target in non-Gaussian clutter. First, a parametric measurement model of reflected signal is developed and a clutter model is described by a SIRV, in which the texture is assumed to be range dependent. Next, considering the heavy computational cost of the NP detector and lack of the prior knowledge of the texture, we concentrated on the performance of GLRT detector, by replacing the unknown quantities with their ML estimates in the likelihood ratio test. The performance of the GLRT detector is determined by the number of subcarriers and sampling pulses, the shape parameter of K-distributed clutter, the SCR, the CNR in a clutter-dominant scenario, and obviously, the detection threshold. We also showed that the GLRT detector has CFAR property, or even if it is not perfectly CFAR, it is very robust (i.e. insensitive to the shape parameter and the mean value in K-distributed clutter). Furthermore, we compared our proposed GLRT detector with some other detectors. However, we cannot directly take advantage of these detectors because of the dimensional limitation of OFDM signal. The numerical results show that range and Doppler designed detector has a remarkable performance gain, compared with range-only designed detector and point target detector in non-Gaussian clutter. Nevertheless, the detection performance has merely a slight gain for range and Doppler designed detector in Gaussian clutter. In addition, we addressed an adaptive waveform design method to optimize the transmitted weights for the next CPI, giving rise to a performance gain (approximately 2dB) as the average output of SCR is increased in comparison to the fixed transmit weights system.

REFERENCES

[1] S. Weinstein and P. Ebert, "Data transmission by frequency-division multiplexing using the discrete Fourier transform," *IEEE Trans. Commun. Technol.*, vol. COM-19, no. 5, pp. 628–634, Oct. 1971.
[2] N. Levanon and E. Mozeson, *Radar Signals*. Hoboken, NJ, USA: Wiley, 2004.

[3] G. E. A. Franken, H. Nikookar, and P. V. Genderen, "Doppler tolerance of OFDM-coded radar signals," in *Proc. Eur. Radar Conf.*, Manchester, U.K., 2006, pp. 108–111.
[4] S. Sen and A. Nehorai, "Adaptive design of OFDM radar signal with improved wideband ambiguity function," *IEEE Trans. Signal Process*, vol. 58, no. 2, pp. 928–933, Feb. 2010.
[5] S. Sen and A. Nehorai, "Target detection in clutter using adaptive OFDM radar," *IEEE Signal Process. Lett*, vol. 16, no. 7, pp. 592–595, Jul. 2009.
[6] S. Sen and A. Nehorai, "Adaptive OFDM radar for target detection in multipath scenarios," *IEEE Trans. Signal Process*, vol. 59, no. 1, pp. 78–90, Jan. 2011.
[7] S. Sen and A. Nehorai, "OFDM MIMO radar with mutual-information waveform design for low-grazing angle tracking," *IEEE Trans. Signal Process*, vol. 58, no. 6, pp. 3152–3162, Jun. 2010.
[8] Y. Xia, Z. Song, Z. Lu, and Q. Fu, "Optimal OFDM waveform design for extended targets detection," in *Proc. Int. Congr. Image Signal Process*, 2015, pp. 1469–1473.
[9] D. Garmatyuk and M. Brenneman, "Adaptive multicarrier OFDM SAR signal processing," *IEEE Trans. Geosci. Remote Sens.*, vol. 49, no. 10, pp. 3780–3790, Oct. 2011.
[10] C. Sturm and W. Wiesbeck, "Waveform design and signal processing aspects for fusion of wireless communications and radar sensing," *Proc. IEEE*, vol. 99, no. 7, pp. 1236–1259, Jul. 2011.
[11] Y. L. Sit, C. Sturm, T. Zwick, L. Reichardt, and W. Wiesbeck, "The OFDM joint radar-communication system: An overview," in *Proc. SPACOMM*, Budapest, Hungary, 2011, pp. 69–74.
[12] Y. Liu, G. Liao, J. Xu, Z. Yang, and Y. Zhang, "Adaptive OFDM integrated radar and communications waveform design based on information theory," *IEEE Commun. Lett*, vol. 21, no. 10, pp. 2174–2177, Oct. 2017.
[13] G. Hakobyan and B. Yang, "A novel intercarrier-interference free signal processing scheme for OFDM radar," *IEEE Trans. Veh. Technol*, vol. 67, no. 6, pp. 5158–5167, Jun. 2017.
[14] Y. Xia, Z. Song, Z. Lu, and Q. Fu, "Target detection in compound-Gaussian clutter with adaptive OFDM radar," *Prog. Electromagn. Res.*, vol. 45, pp. 91–99, 2016.
[15] S. Kay, "Optimal signal design for detection of Gaussian point targets in stationary Gaussian clutter/reverberation," *IEEE J. Sel. Topics Signal Process.*, vol. 1, no. 1, pp. 31–41, Jun. 2007.
[16] E. Conte, A. D. Maio, and G. Ricci, "CFAR detection of distributed targets in non-Gaussian disturbance," *IEEE Trans. Aerosp. Electron. Syst.*, vol. 38, no. 2, pp. 612–621, Apr. 2002.
[17] E. Conte and M. Longo, "Characterisation of radar clutter as a spherically invariant random process," *IEE Proc. F-Commun., Radar Signal Process.*, vol. 134, no. 2, pp. 191–197, Apr. 1987.
[18] N. Bon, A. Khenchaf, and R. Garello, "GLRT subspace detection for range and Doppler distributed targets," *IEEE Trans. Aerosp. Electron. Syst.*, vol. 44, no. 2, pp. 678–696, Apr. 2008.
[19] E. Conte, M. Lops, and G. Ricci, "Adaptive matched filter detection in spherically invariant noise," *IEEE Signal Process. Lett.*, vol. 3, no. 8, pp. 248–250, Aug. 1996.
[20] E. Conte, M. Lops, and G. Ricci, "Asymptotically optimum radar detection in compound-Gaussian clutter," *IEEE Trans. Aerosp. Electron. Syst.*, vol. 31, no. 2, pp. 617–625, Apr. 1995.
[21] F. Gini, "Sub-optimum coherent radar detection in a mixture of K-distributed and Gaussian clutter," *IEE Proc.–Radar, Sonar Navigat.*, vol. 144, no. 1, pp. 39–48, Feb. 1997.
[22] F. Gini and A. Farina, "Vector subspace detection in compound-Gaussian clutter. Part I: Survey and new results," *IEEE Trans. Aerosp. Electron. Syst.*, vol. 38, no. 4, pp. 1295–1311, Oct. 2002.
[23] F. Gini and A. Farina, "Matched subspace CFAR detection of hovering helicopters," *IEEE Trans. Aerosp. Electron. Syst.*, vol. 35, no. 4, pp. 1293–1305, Oct. 1999.
[24] F. Gini and M. V. Greco, "Suboptimum approach to adaptive coherent radar detection in compound-Gaussian clutter," *IEEE Trans. Aerosp. Electron. Syst.*, vol. 35, no. 3, pp. 1095–1104, Jul. 1999.
[25] K. J. Sangston, F. Gini, M. V. Greco, and A. Farina, "Structures for radar detection in compound Gaussian clutter," *IEEE Trans. Aerosp. Electron. Syst.*, vol. 35, no. 2, pp. 445–458, Apr. 1999.
[26] K. Gerlach, "Spatially distributed target detection in non-Gaussian clutter," *IEEE Trans. Aerosp. Electron. Syst.*, vol. 35, no. 3, pp. 926–934, Jul. 1999.
[27] H. Van Trees, Detection, *Estimation, and Modulation Theory. Part III*. New York, NY, USA: Wiley, 1971.
[28] S. Kay, *Fundamentals of Statistical Signal Processing: Detection Theory*. vol. 2. Upper Saddle River, NJ, USA: Prentice-Hall, 1998.
[29] T. Coleman, M. Branch, and A. Grace, "Optimization toolbox: For use with MATLAB, Ver. 2," MathWorks, Natick, MA, USA, Tech. Rep., 1999.
[30] M. Grant and S. Boyd. (Oct. 2010). *CVX: MATLAB Software for Disciplined Convex Programming, Version 1.21*. [Online]. Available: http://cvxr.com/cvx

ZHEN DU was born in Hefei, Anhui, China, in 1993. He received the B.Sc. degree in communication engineering from Northwestern Polytechnical University, Xi'an, China, in 2016. He is currently pursuing the Ph.D. degree with the Department of Electronic Engineering, Shanghai Jiao Tong University, Shanghai, China. His research interests include target detection and waveform design theory.

ZENGHUI ZHANG (M'13) received the B.Sc. degree in applied mathematics, the M.Sc. degree in computational mathematics, and the Ph.D. degree in information and communication engineering from the National University of Defense Technology (NUDT), Changsha, China, in 2001, 2003, and 2008, respectively. From 2008 to 2012, he was a Lecturer with the Department of Mathematics and System Science, NUDT. He is currently an Associate Professor with the School of Electronic Information and Electrical Engineering, Shanghai Jiao Tong University, Shanghai, China. His research interests include radar signal processing and compressed sensing theory and applications.

WENXIAN YU was born in Shanghai, China, in 1964. He received the B.Sc. degree in radio measurement and control and data transmission, the M.Sc. degree in communication and electronic system, and the Ph.D. degree in communication and information system from the National University of Defense Technology (NUDT), Changsha, China, in 1985, 1988, and 1993, respectively. From 1996 to 2008, he was a Professor with the College of Electronic Science and Engineering, NUDT, where he served as the Deputy Head of the College and the Assistant Director of the National Key Laboratory of Automatic Target Recognition. From 2009 to 2011, he was the Executive Dean with the School of Electronic Information and Electrical Engineering, Shanghai Jiao Tong University, Shanghai, where he is currently a Yangtze River Scholar Distinguished Professor. His research interests include radar target recognition, remote sensing information processing, multisensor data fusion, and integrated navigation systems. He has published over 200 research papers in these areas.